Pergamon

Cement and Concrete Research 32 (2002) 915–921

CEMENT AND CONCRETE RESEARCH

# Mechanism of sulfate attack: A fresh look
## Part 1: Summary of experimental results

Manu Santhanam, Menashi D. Cohen*, Jan Olek

*School of Civil Engineering, Purdue University, 1284 Civil Engineering Building, G217, West Lafayette, IN 47907, USA*

Received 24 September 2001; accepted 18 December 2001

## Abstract

This paper reports the results of an investigation on the effects of sodium and magnesium sulfate solutions on expansion and microstructure of different types of Portland cement mortars. The effects of using various sulfate concentrations and of using different temperatures are also reported. The results suggest that the expansion of mortars in sodium sulfate solution follows a two-stage process. In the initial stage, Stage 1, there is little expansion. This is followed by a sudden and rapid increase in the expansion in Stage 2. Microstructural studies suggest that the onset of expansion in Stage 2 corresponds to the appearance of cracks in the chemically unaltered interior of the mortar. Beyond this point, the expansion proceeds at an almost constant rate until the complete deterioration of the mortar specimen. In the case of magnesium sulfate attack, expansion occurs at a continually increasing rate. Microstructural studies suggest that a layer of brucite (magnesium hydroxide) on the surface forms almost immediately after the introduction of the specimens into the solution. The attack is then governed by the steady diffusion of sulfate ions across the brucite surface barrier. The ultimate failure of the specimen occurs as a result of the decalcification of the calcium silicate hydrate (C-S-H), and its conversion to magnesium silicate hydrate (M-S-H), after prolonged exposure to the solution. The effects of using various admixtures, and of changing the experimental variables such as the temperature and concentration of the solution, are also summarized in this paper. Models for the mechanism of the attack resulting from sodium and magnesium sulfate solutions will be presented in Part 2. © 2002 Published by Elsevier Science Ltd.

*Keywords:* Expansion; Microstructure; SEM; Sulfate attack; Mechanism

## 1. Introduction

The general reactions involved in external sulfate attack have been described previously by Cohen and Bentur [1]. Sulfate attack on cement mortars or concrete leads to the conversion of the hydration products of cement to ettringite, gypsum, and other phases, and also to the destabilization of the primary strength providing calcium silicate hydrate (C-S-H) gel. The formation of ettringite and gypsum is common in cementitious systems exposed to most types of sulfate solutions. The expansion resulting from sulfate attack is generally attributed to the formation of these two compounds, although there is some controversy surrounding the exact mechanisms causing expansion [2–4]. When the attacking solution contains magnesium ion, such as in magnesium sulfate ($MgSO_4$), the formation of magnesium hydroxide (brucite) and the conversion of C-S-H into magnesium silicate hydrate (M-S-H) are also observed [5].

The alteration of microstructure of concrete damaged by sulfate attack is described in detail by Diamond and Lee [6]. Several other studies have also successfully used scanning electron microscopy (SEM) to describe the appearance of new phases and the alteration of existing phases of hydrated cement due to the action of sulfates [7,8].

The study reported in this paper is unique in the sense that microstructural studies were performed in conjunction with the measurement of physical properties, such as length change, mass change, loss in strength and dynamic modulus, and chemical analyses using thermal analysis methods such as differential scanning calorimetry (DSC). This article presents the analysis of the results of length change and microscopy studies of cementitious mortars subjected to attack by sodium and magnesium sulfate solutions. The results related to other studies are reported by Santhanam [9].

In Part 2 of the paper, the observed experimental results have been consolidated into a single model to explain the

---

* Corresponding author. Tel.: +1-765-494-5018; fax: +1-765-496-1364.
*E-mail address*: mcohen@ecn.purdue.edu (M.D. Cohen).

0008-8846/02/$ – see front matter © 2002 Published by Elsevier Science Ltd.
PII: S0008-8846(02)00724-X

mechanism of failure of cementitious mortars subjected to attack by sodium and magnesium sulfate solutions.

## 2. Experimental methods and materials

The effect of the following variables on the expansion of cementitious mortars, and the alteration of the microstructure of the mortar due to exposure to sodium and magnesium sulfate solutions, was included in this investigation:

- Air entrainment
- Replacement of cement by silica fume (SF) and metakaolin (MK)
- Use of sodium citrate as a chemical admixture
- Temperature of the sulfate solution
- Concentration of the sulfate solution

The composition and physical properties of the cement (PC), SF, and MK used in the study are presented in Table 1.

The air-entraining agent used was a sodium salt of tall oil resins, and had a solids content of 11%. The dosage used was 0.08% by mass of cement. Reagent grade sodium citrate powder was used as an admixture at the dosage of 0.4% by mass of cement. The study of sodium citrate was included in an attempt to reduce the expansion caused by gypsum formation, since it has been reported [10] that the crystal habit of gypsum is modified in the presence of sodium citrate. Gypsum normally crystallizes in needle-shaped form with numerous air voids (which could be a reason for the expansion caused by gypsum), but in the presence of sodium citrate, gypsum nucleates in a short stubby form. Sodium citrate is also an effective set retarder for cement. Thus, the study of its effects on the sulfate resistance could also provide some insight into the influence of retarders.

Mortars were prepared according to the mixture proportions defined in ASTM C-109 [11] and mixing procedures defined in ASTM C-305 [12]. The composition of these mortars is presented in Table 2.

Mortar prisms (6 × 15 × 80 mm) with acrylic end pieces, as described by Richards and Helmuth [13] (with some minor modifications done at Purdue University) were used for length measurements. Fig. 1 shows the details of the end pieces. SEM studies were performed on 1/2-in. thick slices from 23 × 80 mm cylindrical specimens.

Table 1
Composition and physical properties of cementitious materials

| Property | Type I PC | SF | MK |
|---|---|---|---|
| CaO (%) | 64.60 | 0.15 | – |
| $SiO_2$ (%) | 20.63 | 98.25 | 53.79 |
| $Al_2O_3$ (%) | 5.03 | Trace | 46.15 |
| $Fe_2O_3$ (%) | 2.80 | Trace | Trace |
| $C_3S$ (%) | 62.00 | – | – |
| $C_3A$ (%) | 9.00 | – | – |
| $SO_3$ (%) | 2.67 | – | – |
| Alkalis (%) | 0.50 | – | – |
| Fineness ($cm^2/g$) | 3600 | 20,000 | 5500 |
| Specific gravity | 3.15 | 2.20 | 2.45 |

Table 2
Composition of mortars prepared for the study

| Designation | % Composition | | | | Water to binder ratio | Admixture |
|---|---|---|---|---|---|---|
| | Type I PC | $C_3S$ | SF | MK | | |
| PC | 100 | – | – | – | 0.485 | – |
| PC-N | 100 | – | – | – | 0.485 | Na-Citrate |
| AE | 100 | – | – | – | 0.460 | AEA |
| SF | 90 | – | 10 | – | 0.600 | – |
| MK | 80 | – | – | 20 | 0.600 | – |

The mortar specimens were removed from their molds 1 day after mixing, and then stored in saturated limewater solution for an additional 13 days. After the initial curing, the initial length was measured, and the specimens were then transferred to the respective solutions. The details of the temperature and concentrations of the various solutions used are presented in Table 3. PC mortars were immersed in all solutions listed in the table. The modified mortars were only immersed in LW, NS1 and MS1, at a temperature of 70 °F (± 3 °F) (see definitions in Table 3).

Length measurements were conducted periodically. The data presented in the figures in this article are the average expansions for three sets of measurements. SEM studies were performed after 12 weeks of immersion in the solutions.

The specimens used for SEM were dried at 70 °C in an oven for 1 day, and then embedded in a low-modulus epoxy. The specimens were then polished using progressively finer grids, and then coated with a gold–palladium coating.

## 3. Results

### 3.1. Experimental results for PC mortars

#### 3.1.1. Expansion

The expansion of mortar bars exposed to sodium sulfate solution, as shown in Fig. 2, occurs in two stages, which agrees with the results of a previous study by Clifton et al.

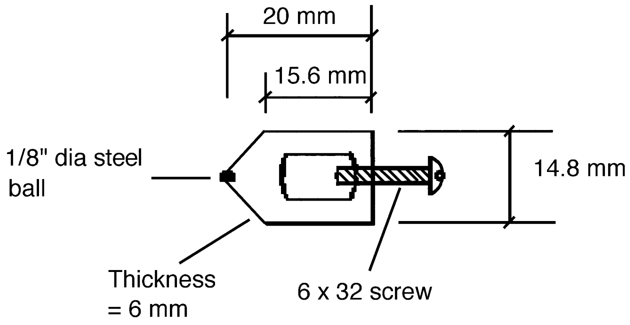

Fig. 1. Details of the acrylic end piece used in the mortar specimens for length measurements.

Table 3
Details of attacking solutions used in the study

| Designation | Solution | Strength | Equivalent $SO_3$ (ppm) | Equivalent $Mg^{2+}$ (ppm) | Storage temperature (°F) |
|---|---|---|---|---|---|
| LW | Limewater | Saturated | – | – | 40, 70, 85, 100 |
| NS1 | Sodium sulfate | 4.500% | 25 000 | – | 40, 70, 85, 100 |
| NS2 | Sodium sulfate | 2.250% | 12 500 | – | 70 |
| NS3 | Sodium sulfate | 1.125% | 6250 | – | 70 |
| NS4 | Sodium sulfate | 0.563% | 3125 | – | 70 |
| NS5 | Sodium sulfate | 0.281% | 1562 | – | 70 |
| MS1 | Magnesium sulfate | 3.800% | 25 000 | 7600 | 40, 70, 85, 100 |
| MS2 | Magnesium sulfate | 1.900% | 12 500 | 3800 | 70 |
| MS3 | Magnesium sulfate | 0.950% | 6250 | 1900 | 70 |
| MS4 | Magnesium sulfate | 0.475% | 3125 | 950 | 70 |
| MS5 | Magnesium sulfate | 0.237% | 1562 | 475 | 70 |

[14]. In Stage 1, the expansion is very low, and this stage can thus be called the 'induction period'. At the end of this induction period, expansion increases suddenly and then proceeds at a steady rate until the specimen disintegrates.

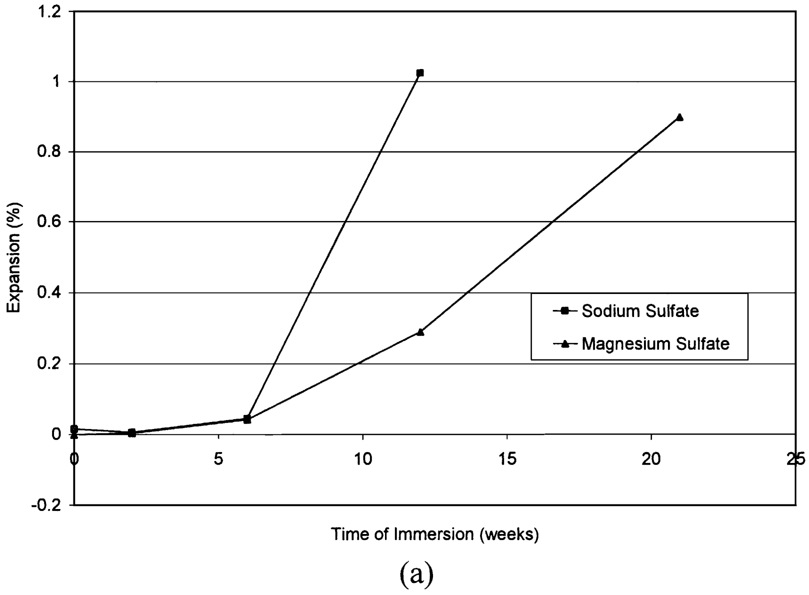

(a)

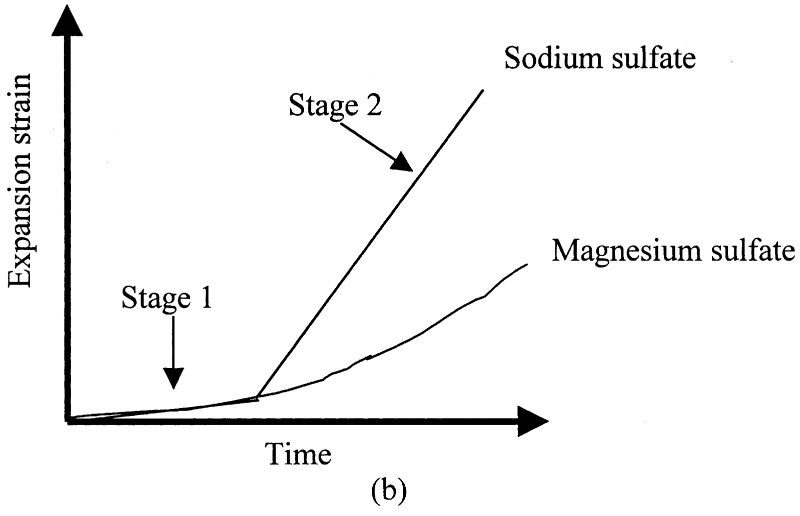

(b)

Fig. 2. Observed (a) and idealized (b) expansion behavior of PC mortars stored in sodium and magnesium sulfate solutions; Stage 1 and Stage 2 are marked for the expansion behavior in sodium sulfate solution.

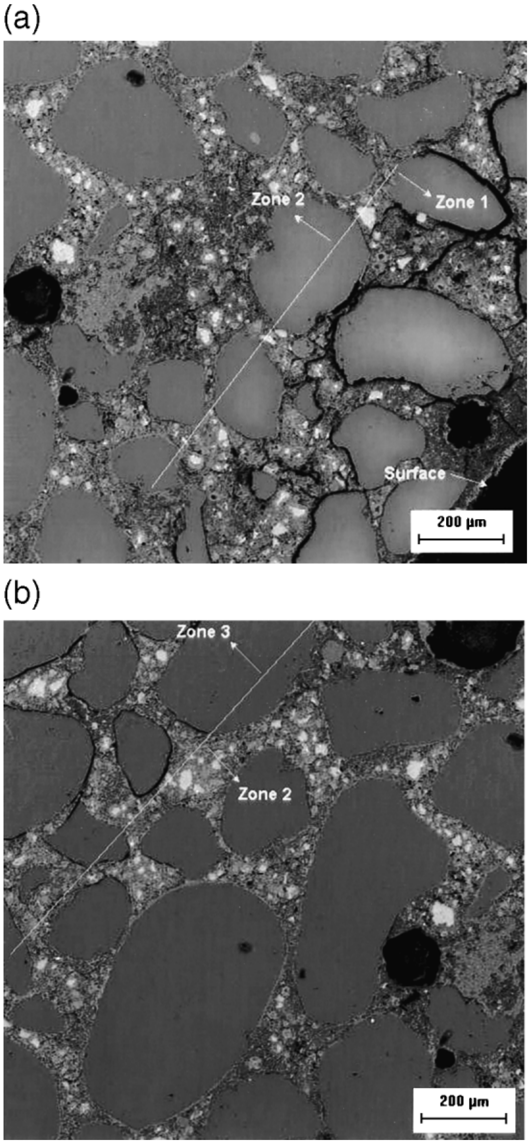

Fig. 3. (a, b): PC mortar specimen stored in sodium sulfate solution for 12 weeks, showing formation of distinct zones parallel to the surface.

This stage has been marked Stage 2. This two-stage expansion behavior for sodium sulfate attack is also evident in other research studies [15,16]. It is speculated that the sudden increase in expansion in Stage 2 occurs due to the increase in the amounts of gypsum and ettringite over that which can be accommodated by the mortar structure. A detailed analysis is presented in Part 2.

On the other hand, the expansion of mortars stored in magnesium sulfate solution occurs at a continually increasing rate, as shown in Fig. 2. Results from thermal analyses by DSC, which are not included here but have been reported elsewhere [9], indicate that a layer of brucite formed on the surface of the mortars soon after immersion into the solution. The steady increase in the rate of expansion can be most likely attributed to the diffusion of sulfate ions across this layer of brucite.

### *3.1.2. Microstructural observations by SEM*

The mortars attacked by sodium sulfate also exhibit a peculiar crack pattern, which occurs as a direct result of the mechanism by which the attack takes place. The microstructure of attacked mortars, presented in the micrographs in Figs. 3–6, shows a disintegrated surface zone (Zone 1), followed by a zone of deposition of attack products (Zone 2), followed by the interior of the mortar (Zone 3), which shows the appearance of microcracks (as indicated by the presence of narrow dark bands around the aggregates), although chemically unaltered. The details of the microstructure in each of these zones are presented in Figs. 4, 5 and 6, for Zones 1, 2 and 3, respectively.

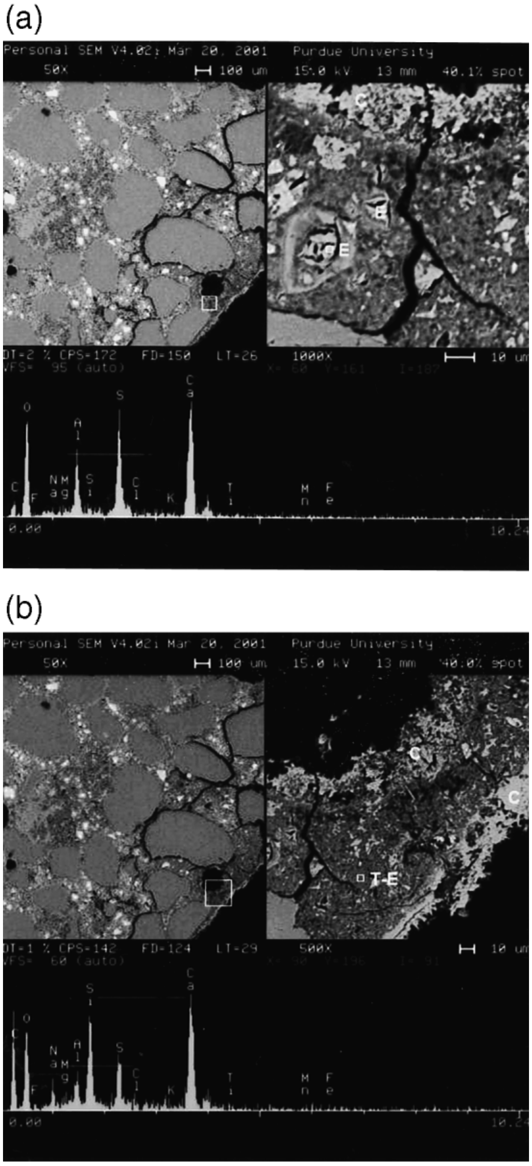

Fig. 4. (a, b): Details of Zone 1 in the PC mortar specimen stored in sodium sulfate solution for 12 weeks; the dark paste represents decalcified C-S-H, deposits of ettringite (E) and thaumasite–ettringite solid solutions (T–E) can be observed under a surface layer of calcite (C).

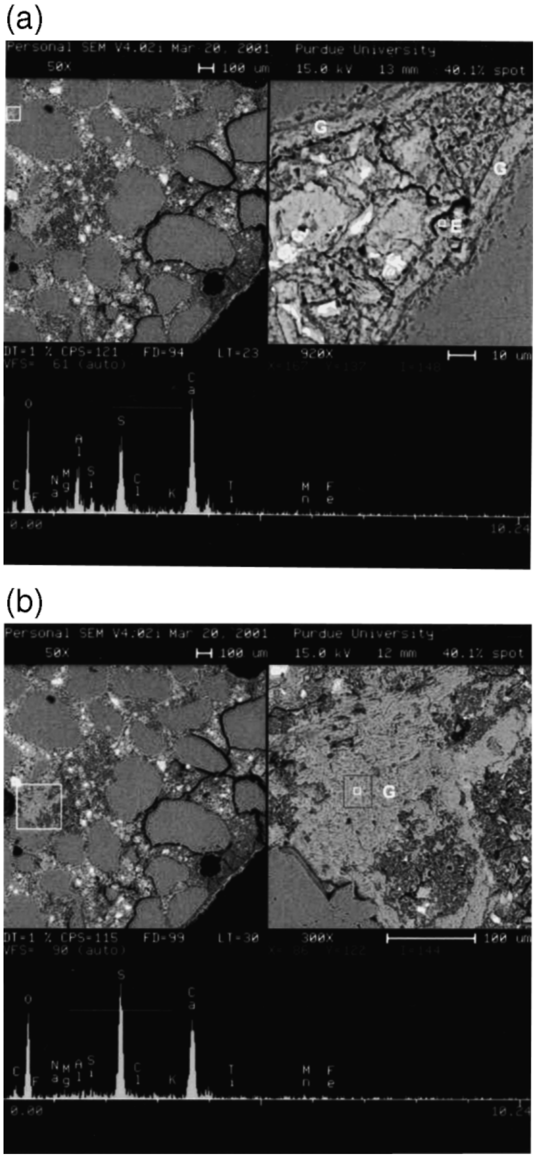

Fig. 5. (a, b): Details of Zone 2 in the PC mortar specimen stored in sodium sulfate solution for 12 weeks; abundant deposition of gypsum (G) in the paste as well as around the aggregates is observed, and deposits of ettringite (E) are also seen.

The SEM micrographs of PC mortars stored in magnesium sulfate solution are presented in Figs. 7 and 8. The presence of the brucite–gypsum double layer at the surface is evident. Formation of M-S-H is limited, even after prolonged immersion, to the regions close to the surface where the brucite layer is cracked or depleted. Secondary gypsum is also detected near the M-S-H deposits.

### 3.2. Summary of the effects of the variables

### 3.2.1. Expansion of mortars

*3.2.1.1. Effects of air entrainment.* The overall expansion of mortars for the air-entrained (AE) mortars was similar to the non-AE PC mortars, in both sodium and magnesium sulfate solutions. The duration of Stage 1 was also similar in both cases. However, the visual deterioration of the AE specimens was less pronounced.

*3.2.1.2. Effects of pozzolanic substitution.* In sodium sulfate, the expansion was drastically reduced in the pozzolan-substituted mortars. The length of the initial period (Stage 1) was also increased. In magnesium sulfate, although the overall expansion was reduced for both SF and MK mortars compared to the PC mortars, the deterioration level of MK mortars specimens was high, and complete disintegration of the specimens occurred after 32 weeks. SF mortar performed better than the PC mortar. Visual deterioration was not as pronounced as the PC mortar, and the expansion was also lower for the SF mortar.

*3.2.1.3. Effects of using sodium citrate.* In both sodium and magnesium sulfate solutions, the overall expansion resulting from the use of sodium citrate was reduced. In sodium sulfate solution, the duration of Stage 1 was increased, indicating a delay in the onset of expansion. In magnesium sulfate, the expansion was reduced drastically, to almost one third of the PC mortar.

*3.2.1.4. Effects of increasing temperature of the attacking solution.* An increase in the temperature of the solution led to a decrease in the length of the initial period (Stage 1) for the mortars stored in sodium sulfate solution. During Stage 2, the rate of expansion was similar at all the temperatures. In the case of the magnesium sulfate solution, the increase in temperature led to an increase of the rate of expansion of the mortars.

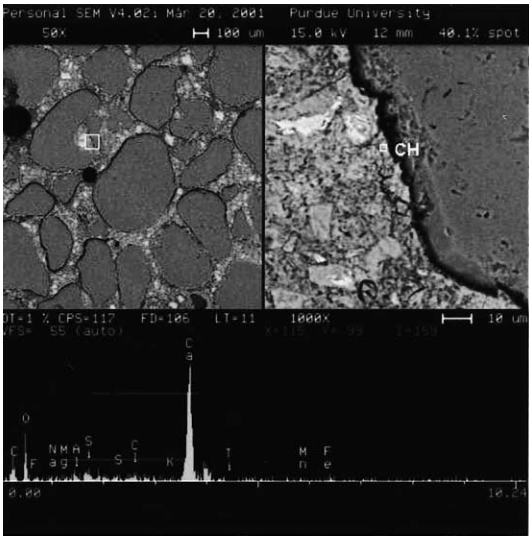

Fig. 6. Details of Zone 3 in the PC mortar specimen stored in sodium sulfate solution for 12 weeks; the paste appears normal (energy dispersive X-ray analysis confirmed that this region was chemically unaltered), and deposits of calcium hydroxide (CH) are seen around the aggregate.

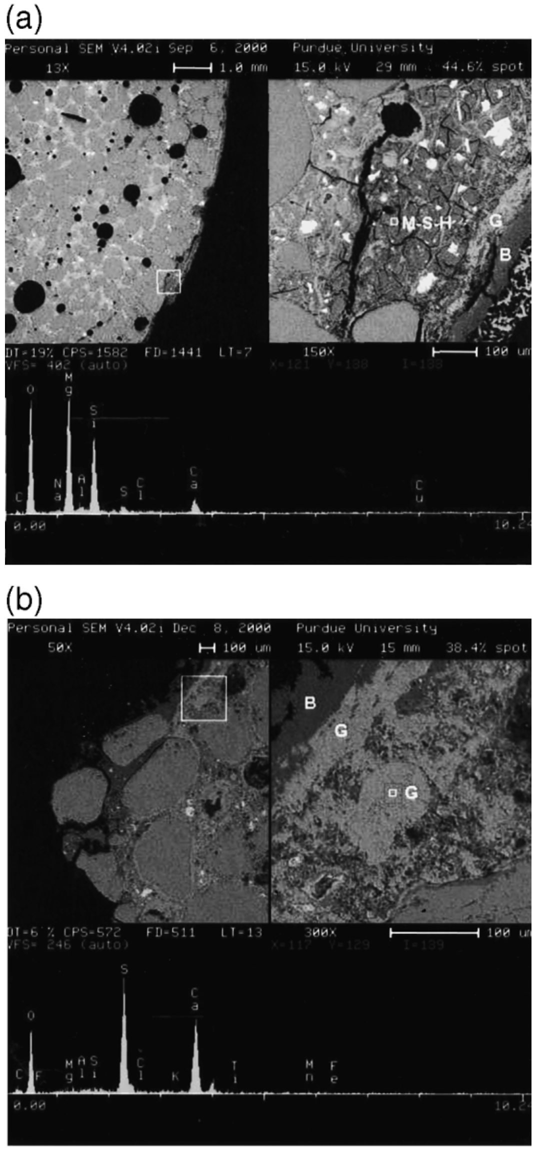

Fig. 7. (a, b): Surface region of the PC mortar stored in magnesium sulfate solution for (a) 12 weeks, and (b) 32 weeks; even at 32 weeks, the surface brucite (B) and gypsum (G) layers are still evident.

*3.2.1.5. Effects of increasing concentration of the attacking solution.* An increase in the concentration of the solution led to an increase of the rate of expansion during Stage 2 for the mortars stored in sodium sulfate solution. The length of the initial period (Stage 1) was similar at all concentrations. In the magnesium sulfate solution, the increase in concentration led to higher rates of expansion.

### 3.2.2. Microstructural observations using SEM

For all the different mortars with admixtures (air-entrainment, SF, MK and sodium citrate), the pattern of deterioration observed under the SEM was similar to the PC mortars, in both solutions of sodium and magnesium sulfates. In the case of AE mortars, the attack products were mainly deposited within the air voids. The MK mortar specimen stored in magnesium sulfate solution showed a complete transformation of the C-S-H to M-S-H and secondary gypsum, which supports the occurrence of complete disintegration and poor performance of MK mortars.

In general, the mortars stored in sodium sulfate solution, showing lower expansions, also showed reduced amount of cracking in the interior zones. In the case of the magnesium sulfate solution, the poorly performing mortars showed greater formation of M-S-H and secondary gypsum.

At increased temperatures and concentrations, the cracking observed in the mortars was higher. In the sodium sulfate solution, the depth of the deteriorated surface zones was also larger at higher temperatures and concentrations. More gypsum was detected in the middle zone (Zone 2) at higher temperatures and concentrations. At the lowest temperature (40 °F), distinct deposits of thaumasite were

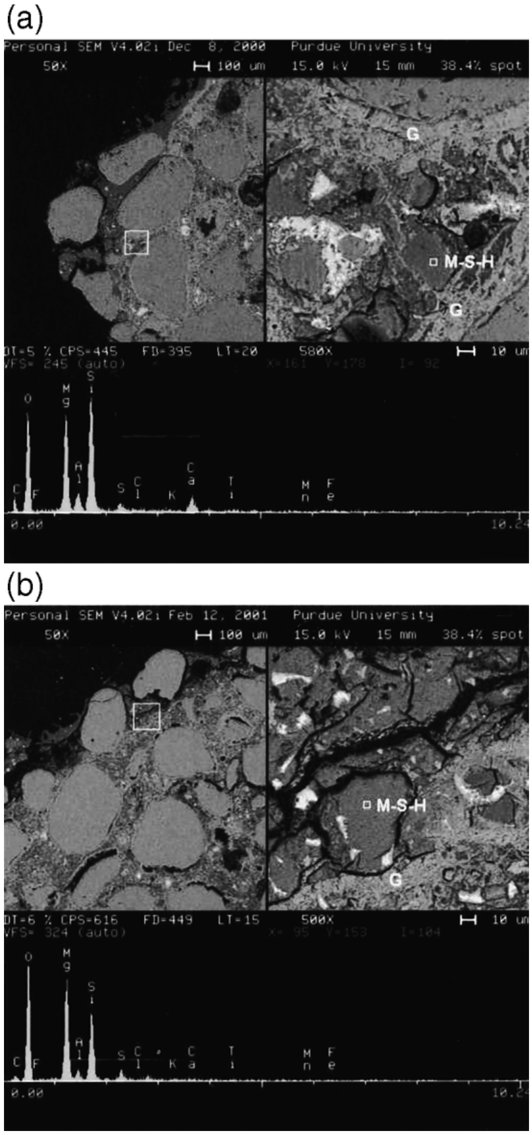

Fig. 8. (a, b): Highly deteriorated regions from the PC mortar specimen stored in magnesium sulfate solution for 32 weeks; the abundant conversion of C-S-H to M-S-H, accompanied by gypsum (G) deposition, is evident.

visible in the near-surface zones. In the case of the magnesium sulfate solution, more M-S-H and gypsum were detected at higher temperatures and concentrations.

## 4. Summary

The results of experiments monitoring the length change of cementitious mortars subject to attack by sodium and magnesium sulfate solutions are presented in this paper, along with microstructural observations using SEM.

Expansion of mortar specimens in sodium sulfate solution follows a two-stage process, where an initial stage (Stage 1) of very low expansion is followed by a sudden increase in the expansion (Stage 2). In this second stage of expansion, the rate of expansion is nearly constant until failure. On the other hand, expansion in magnesium sulfate solution occurs at a continuously increasing rate.

Observations from SEM studies indicate the formation of various zones within the attacked mortar. In the sodium sulfate solution, three distinct zones are formed. A cracked and highly deteriorated surface zone (Zone 1) is followed by a zone of deposition of attack products (Zone 2), primarily gypsum around aggregates and in pores, and ettringite within the paste. This is followed by the interior chemically unaltered zone (Zone 3) which is cracked. In the magnesium sulfate solution, a surface double layer of brucite and gypsum provides a barrier to the free passage of the external solution to the interior of the mortar. Gypsum and ettringite are deposited just under this surface layer of brucite. In highly deteriorated areas, where the brucite layer is cracked, the conversion of C-S-H to M-S-H takes place.

The effects of using various admixtures, as well as of changing the concentration and temperature of the sulfate solution, have also been presented in this paper. Results indicate that the pattern of deterioration and the type of reaction products formed are similar in most of the cementitious mortar systems. The parameters that change are only the total expansion and the time to deterioration.

## Acknowledgments

The Andrews Fellowship from Purdue University is gratefully acknowledged. Insightful comments and suggestions from Dr. Jason Weiss and Dr. Sidney Diamond at Purdue University are also appreciated.

## References

[1] M.D. Cohen, A. Bentur, Durability of Portland cement–silica fume pastes in magnesium sulfate and sodium sulfate solutions, ACI Mater. J. 85 (3) (1988) 148–157.

[2] M.D. Cohen, Theories of expansion in sulfoaluminate-type expansive cements: Schools of thought, Cem. Concr. Res. 13 (1983) 809–818.

[3] P.W. Brown, H.F.W. Taylor, The role of ettringite in external sulfate attack, in: J. Skalny, J. Marchand (Eds.), Material Science of Concrete — Sulfate Attack Mechanisms, American Ceramic Society, Westerville, OH, 1999, pp. 73–98.

[4] W.C. Hansen, Crystal growth as a source of expansion in Portland cement concrete, Proc. ASTM 63.

[5] D. Bonen, M.D. Cohen, Magnesium sulfate attack on Portland cement paste: I. Microstructural analysis, Cem. Concr. Res. 22 (1992) 169–180.

[6] S. Diamond, R.J. Lee, Microstructural alterations associated with sulfate attack in permeable concretes, in: J. Skalny, J. Marchand (Eds.), Material Science of Concrete—Sulfate Attack Mechanisms, American Ceramic Society, Westerville, OH, 1999, pp. 123–174.

[7] R.S. Gollop, H.F.W. Taylor, Microstructural and microanalytical studies of sulfate attack: I. Ordinary Portland cement paste, Cem. Concr. Res. 22 (1992) 1027–1038.

[8] D. Bonen, Composition and appearance of magnesium silicate hydrate and its relation to deterioration of cement based materials, J. Am. Ceram. Soc. 75 (10) (1992) 2904–2906.

[9] M. Santhanam, Studies on Sulfate Attack: Mechanisms, Test Methods, and Modeling, PhD Thesis, Purdue University, August 2001.

[10] F.M. Lea, R. Nurse, Problems of crystal growth in building materials, Crystal Growth—Discussions of The Faraday Society, No. 5, Royal Society of Chemistry, London, 1949, pp. 345–352.

[11] ASTM Standard Designation C-109, Standard Test Method for Compressive Strength of Hydraulic Cement Mortars, The American Society of Testing and Materials, 1996.

[12] ASTM Standard Designation C-305, Standard Practice for Mechanical Mixing of Hydraulic Cement Pastes and Mortars of Plastic Consistency, The American Society of Testing and Materials, 1996.

[13] C.W. Richards, R.A. Helmuth, Expansive Cement Concrete—Micromechanical Models for Free and Restrained Expansion, Technical Report TR 191, Department of Civil Engineering, Stanford University, Stanford, CA, January 1977, 36 pp.

[14] J.R. Clifton, G. Frohnsdorff, C. Ferraris, Standards for evaluating the susceptibility of cement-based materials to external sulfate attack, in: J. Skalny, J. Marchand (Eds.), Material Science of Concrete — Sulfate Attack Mechanisms, American Ceramic Society, Westerville, OH, 1999, pp. 337–355.

[15] B. Tian, M.D. Cohen, Does gypsum formation during sulfate attack on concrete lead to expansion? Cem. Concr. Res. 30 (2000) 117–123.

[16] K.E. Kurtis, P.J.M. Monteiro, S.M. Madanat, Empirical models to predict concrete expansion caused by sulfate attack, ACI Mater. J. 97 (2) (2000) 156–161.